Toxicology Letters 187 (2009) 77–83

Contents lists available at ScienceDirect

Toxicology Letters

journal homepage: www.elsevier.com/locate/toxlet

Oxidative stress of CeO_2 nanoparticles *via* p38-Nrf-2 signaling pathway in human bronchial epithelial cell, Beas-2B

Hyun-Jeong Eom, Jinhee Choi*

Faculty of Environmental Engineering, College of Urban Science, University of Seoul, 90 Jeonnong-dong, Dongdaemun-gu, Seoul 130-743, Republic of Korea

ARTICLE INFO

Article history:
Received 20 August 2008
Received in revised form 22 January 2009
Accepted 23 January 2009
Available online 4 February 2009

Keywords:
CeO_2 nanoparticles
Oxidative stress
p38 MAP kinases
Nrf-2
HO-1

ABSTRACT

To understand the molecular mechanism of previously observed cerium oxide (CeO_2) nanoparticles-induced oxidative stress, an *in vitro* toxicity assay was conducted using human bronchial epithelial cell, Beas-2B, focusing on the involvement of the oxidative stress responding signal transduction pathway and transcription factors in the toxicity of CeO_2 nanoparticles. Extracellular signal-regulating kinase (ERK), p38 and c-Jun N-terminal kinase (JNK) signaling pathways, along with nuclear factor-kappaB (NF-κB) and nuclear factor-E2-related factor-2 (Nrf-2), were investigated as the upstream events of oxidative stress from exposure to CeO_2 nanoparticles. The overall results suggest that CeO_2 nanoparticles may exert their toxicity through oxidative stress, as they cause significant increases in the cellular reactive oxygen species (ROS) concentrations, subsequently leading to the strong induction of heme oxygenase-1 (HO-1) *via* the p38-Nrf-2 signaling pathway. Further studies on the mechanism by which CeO_2 nanoparticles induce the p38-Nrf-2 signaling pathway are warranted for a better understanding of the CeO_2 nanoparticles-induced oxidative stress; studies with other signaling pathways, with concentration–response and time course experiments would also be justified.

1. Introduction

Man-made nanoparticles and materials are being rapidly produced in large quantities throughout the world. Although a wide and growing number of applications for nanomaterials exist, there is a serious lack of information concerning the effects of such manufactured nanomaterials on human health and the environment. Considering their wide range of applications, the impact of nanomaterials on human health and the environment is of great interest. There have been limited studies assessing the toxicity of man-made nanomaterials (Lam et al., 2004; Oberdörster, 2004; Braydich-Stolle et al., 2005; Hussain et al., 2005; Monteiro-Riviere et al., 2005). Of the various manufactured nanomaterials, cerium oxide (CeO_2) has a high potential for widespread use and application. As a lanthanide element oxide, CeO_2 nanoparticles are one of the most important nanomaterials available, finding use in a wide range of applications, including catalysis, solar cells, fuel cells, phosphor/luminescence, abrasives for chemical mechanical planarizations, gas sensors, oxygen pumps and metallurgical and glass/ceramic applications (Murray et al., 1999; Corma et al., 2004; Izu et al., 2004; Zheng et al., 2005).

Although little is known about nanoparticle toxicity, oxidative stress, which elicits a wide variety of cellular events, such as apoptosis, cell cycle arrest and the induction of antioxidant enzymes, has often been reported as nanoparticle-induced toxicity. Numerous previous studies on nanoparticle toxicity, with various cell types and various nanoparticle types, have reported that oxidative stress is one of the most important toxicity mechanisms related to the exposure to nanoparticles (Shvedova et al., 2003; Xia et al., 2004; Green and Howman, 2005; Hussain et al., 2005; Sayes et al., 2005; Foster et al., 2006; Lin et al., 2006; Limbach et al., 2007; Monteiller et al., 2007). Number of studies by other research groups have reported oxidative stress as the toxic mechanism of CeO_2 nanoparticles (Lin et al., 2006; Schubert et al., 2006), as well as in our previous study (Park et al., 2008). In our previous study, the cytotoxicity and oxidative stress caused by CeO_2 nanoparticles were investigated in cultured human bronchial epithelial cells, Beas-2B. Increases in reactive oxygen species (ROS), decreases in GSH, and the inductions of oxidative stress-related genes and apoptosis were observed in cells exposed to CeO_2 nanoparticles.

To understand the observed molecular mechanism of CeO_2 nanoparticles-induced oxidative stress (Park et al., 2008), an *in vitro* toxicity assay was conducted focusing on the involvement of the oxidative stress responding signal transduction pathway and transcription factors in the toxicity of CeO_2 nanoparticles. The upstream signaling mechanism responsible for regulating oxidative stress was studied focusing on the mitogen-activated protein (MAP) kinase cascades (Kyriakis and Avruch, 2001; Takeda et al., 2003).

* Corresponding author. Tel.: +82 2 2210 5622; fax: +82 2 2244 2245.
E-mail address: jinhchoi@uos.ac.kr (J. Choi).

0378-4274/$ – see front matter © 2009 Published by Elsevier Ireland Ltd.
doi:10.1016/j.toxlet.2009.01.028

Three groups of well-characterized MAP kinase cascades, extracellular signal-regulating kinase (ERK), p38 and c-Jun N-terminal kinase (JNK), were investigated. The upstream signaling mechanism responsible for regulating the oxidative stress involved in nanotoxicity is still poorly defined. The MAP kinase cascades are multi-functional signaling pathways, which are evolutionally well conserved in all eukaryotic cells. Three MAP kinase cascades converge on ERKs, JNKs, and p38 MAP kinases have already been characterized (Kyriakis and Avruch, 2001; Takeda et al., 2003). Two of these three MAP kinase cascades converge on JNKs and p38 MAP kinases are preferentially activated by cytotoxic stresses, such as X-ray/UV irradiation, heat/osmotic shock, and oxidative/nitrosative stress (Hagemann and Blank, 2001; Qadri et al., 2004; Camacho-Barquero et al., 2007).

Redox-sensitive transcription factors, such as nuclear factor-kappaB (NF-κB) and nuclear factor-E2-related factor-2 (Nrf-2), were investigated as target transcription factors of CeO_2 nanoparticles toxicities. NF-κB, activated by oxidative stress, induces the expression of a variety of proteins that function in the immunological and cellular detoxifying defense systems (Janssen et al., 1995; Pinkus et al., 1996), and has been identified as a transcription factor regulated by the intracellular redox status (Sen and Packer, 1996). When activated by oxidative stress, Nrf-2 breaks free from Kelch-like ECH-associated protein1 (Keap1) and translocates into the nucleus, where it binds to an antioxidant response element (ARE), a cis-acting enhancer sequence that mediates the transcriptional activation of genes in response to oxidative stress, including heme oxygenase-1 (HO-1, Itoh et al., 2003). In recent years, many studies have reported that the transcription factor Nrf-2 plays an essential role in the ARE-mediated expression of phase II detoxifying and antioxidant enzymes, as well as other stress-inducible genes, in response to oxidative or electrophilic stress (Itoh et al., 1997; Chan and Kan, 1999; Hayes et al., 2000; Chan et al., 2001; Kim et al., 2001; Kwak et al., 2002).

In nanotoxicology, the particle size and surface area are considered important factors in determining toxicity (Oberdörster et al., 2005). Conversely to our previous study, where cells were exposed to different concentrations (5, 10, 20, 40 μg/mL) of 30 nm CeO_2 nanoparticles, in this study the cells were exposed to different sizes (15, 30 and 45 nm) of CeO_2, with the aim of identifying a relationship between the nanoparticle size and toxicity.

2. Materials and methods

2.1. Cell culture and characterization of CeO_2 nanoparticles

Human bronchial epithelial cells, Beas-2B, were maintained in DMEM/F12 (GIBCO BRL Life Technologies, Rockville, MD, USA), supplemented with 10% (v/v) fetal bovine serum and 1% antibiotics, at 37 °C in a humidified atmosphere of air and 5% CO_2. A test solution of CeO_2 nanoparticles, which were synthesized as described previously (Park et al., 2008), was prepared in the DMEM/F12 medium and dispersed for 20 min using a sonicator (Branson Inc., Danbury, CT, USA) to prevent aggregation. During the testing periods, precipitation of nanoparticles was not observed in the culture medium (data not shown). The concentration used in this study was 1 mg/L to prevent aggregation and/or precipitation of particles. The cells were treated with 15, 30 and 45 nm of CeO_2 nanoparticles for 24 h for oxidative stress studies. For surface area measurements, the Branauer, Emmett and Teller (BET) method was used with BELSORP-mini II, a volumetric adsorption apparatus (BEL Japan, Inc., Osaka, Japan). To investigate the size and shape of the CeO_2 nanoparticles, 20 μL of a particle suspension from the test medium was dried on a 400 mesh carbon-coated copper grid and imaged using a JEM 1010 transmission electron microscope (TEM; JEOL, Tokyo, Japan) at 40–100 kV. The size distribution of the nanoparticles was evaluated using a Photal dynamic light scattering (DLS) spectrometer, DLS-7000 (Otsuka Electronics Co., Inc., Osaka, Japan).

2.2. Confocal microscopy, flow cytometry and ROS measurement

Confocal laser scanning microscopy (LSM-510, Carl Zeiss, Baden-Württemberg, Germany) and flow cytometry (FCM, BD Science, San Jose, CA, USA) were used for the analysis of the particles taken up by the cells, in which cells were exposed to 40 mg/L of CeO_2 nanoparticles. FCM was performed for the analysis of the amount of particles taken up by the cells and for apoptosis. The intensities of forward-scattered light (FS) and side-scattered light (SS) are proportional to the size of cells and the intracellular density, respectively. The cell viability was measured using 3-[4,5-dimethylthiazol-2-yl]-2,5-diphenylterazolium bromide (MTT) reagent (Mosmann, 1983), with a 96-well plate reader (TECAN, Hombrechtikon, Switzerland). To detect the generation of ROS in the nanoparticles-treated cells, a fluorometric assay using intracellular oxidation of 2,7-dichlorofluoroscein diacetate (DCFH-DA, Sigma, St. Louis, MO, USA) was performed (Elbekai and El-Kadi, 2005; Fotakis et al., 2005) using a fluorescent microscope (Nikon, Tokyo, Japan), with excitation and emission wavelengths of 485 and 530 nm, respectively.

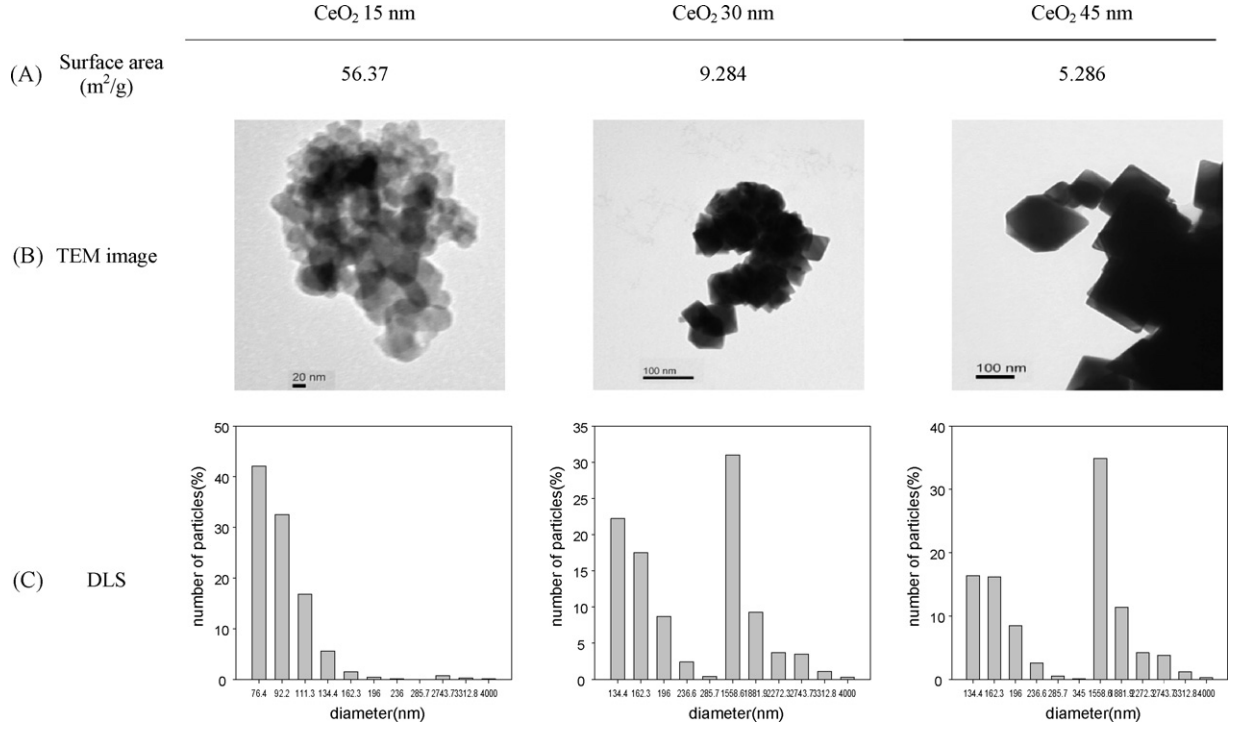

Fig. 1. Characterization of different sized CeO_2 nanoparticles using BET, TEM and DLS methods. Surface areas of nanoparticles were measured using the BET method (A), particle shapes were analyzed by TEM (B) and the size distribution in the test medium by DLS (C).

2.3. Western blotting

Western blotting analysis was performed as described previously (Park et al., 2006) using an enhanced chemiluminescence western blotting detection kit (Amersham, Little Chalfont, Buckinghamshire, UK). Anti-p38 monoclonal-, anti-phospho-p38 monoclonal-, anti-ERK-2 polyclonal-, anti-phospho-ERK monoclonal- and anti-Nrf-2 polyclonal antibodies were purchased from Santa Cruz Biotechnology (Santa Cruz, CA, USA). Anti-JNK polyclonal-, anti-phospho-JNK monoclonal-, anti-NF-κB monoclonal- and anti-I-κB monoclonal antibodies were from Cell Signaling (Beverly, MA, USA). Anti-HO-1 monoclonal antibody was from Stressgen (Victoria, BC, Canada) and anti-Cu/Zn SOD polyclonal antibody was from Biodesign (Saco, ME, USA). Three replicates for each treatment, and a control, were conducted for the western blot analysis. Following the Western blotting, the relative densities of the protein bands were determined using an image analyzer, the Gel Documentation system (Vilber Lourmat TFX-20.M, Marne la Vallee, France), coupled to a Kodak 1D 3.6 camera (Kodak EDAS 290, Rochester, NY, USA).

2.4. Data analysis

Statistical differences between the control and treated cells were examined with the aid of one-way ANOVA test followed by Tukey's test, using SPSS 12.0KO (SPSS Inc., Chicago, Il, USA). An alpha level of 0.05 was used to determine significance in all statistical analyses.

3. Results and discussions

3.1. Characterization of CeO_2 nanoparticles

Prior to the study of the mechanism of oxidative stress, characterization of the CeO_2 nanoparticles was performed using BET, TEM and DLS methods, which provided information on the surface area, morphological shape and size distribution of nanoparticles, respectively (Fig. 1). The BET surface areas for 15, 30 and 45 nm of CeO_2 nanoparticles were 56.3, 9.28 and 5.28 m^3/g, respectively, which suggest the nanoparticles used were of different sizes, as the smaller sized particles have larger surface areas. The TEM images of the CeO_2 nanoparticles from the test medium confirmed that the sizes of the nanoparticles approximately matched the sizes measured after synthesis (15, 30 and 45 nm). The TEM provided information on the size and shape of nanoparticles; however, it could not provide information on whether the nanoparticles existed in single or aggregated forms in the test medium, as the nanoparticles form aggregates when dried on the microscopic observation slide. The size distribution in the test medium, therefore, was investigated using a DLS method, which showed that the main nanoparticle sizes distributed in the test medium were about 76 (for 15 nm of CeO_2) and 1588 nm (for 30 and 45 nm of CeO_2). This suggests that the nanoparticles exposed to the cells did not exist as single particles, but tended to aggregate in the test medium.

The incorporation of CeO_2 nanoparticles was examined using confocal LSM and the FCM-SS analyses (Fig. 2). The confocal LSM images (Fig. 2A) suggested the CeO_2 nanoparticles were incorporated into the cells and distributed around the nucleus area. Fig. 2B shows the FCM light scatter histograms of the cells treated with different CeO_2 nanoparticle sizes (15, 30 and 45 nm). Regardless of treatment with CeO_2 nanoparticles, the value of FS was constant. Conversely, bigger CeO_2 nanoparticles resulted in higher SS intensities; however, this may not have been due to the magnitude of uptake, because if the uptake were the same, the larger particles would be expected to cause more SS. More sophisticated investigations are needed on the characterizations of CeO_2 nanoparticles in test medium (i.e. aggregated- or single forms, intensity of uptake into the cells) and their influence on cytotoxicity. Nevertheless, FCM-SS analysis seems to be used as an initial screening index of "nanotoxicity", as Suzuki et al. (2007) recently reported that this method can provide information about the uptake of nanoparticles into cells. Once the uptake of CeO_2 nanoparticles by the cells had been verified (Fig. 2), for the study of the oxidative stress mechanism, cells were exposed to CeO_2 nanoparticles at a concentration of 1 mg/L. The reason 1 mg/L was selected as the test concentration was because at this concentration, no precipitation of CeO_2 nanoparticles occurred in the test medium during the exposure period, while precipitation did occur at higher concentrations. Moreover, even though this concentration is still very high compared to that in the real environment, it is likely to be more environmentally relevant than the concentrations used in our previous study, where cells were exposed to CeO_2 nanoparticles at up to 40 μg/mL (Park et al., 2008).

3.2. MAP kinase signal transduction and transcription factors

To initially screen the sensitivity of cell to CeO_2 nanoparticles, the cell viability was examined (Fig. 3). Statistically significant decreases in the cell viability were observed with exposure to 30 and 45 nm CeO_2. The formation of ROS was visualized in Beas-2B cells exposed to CeO_2 nanoparticles using inspection under fluorescent microscopy (Fig. 4). DCFH-DA staining revealed an increased

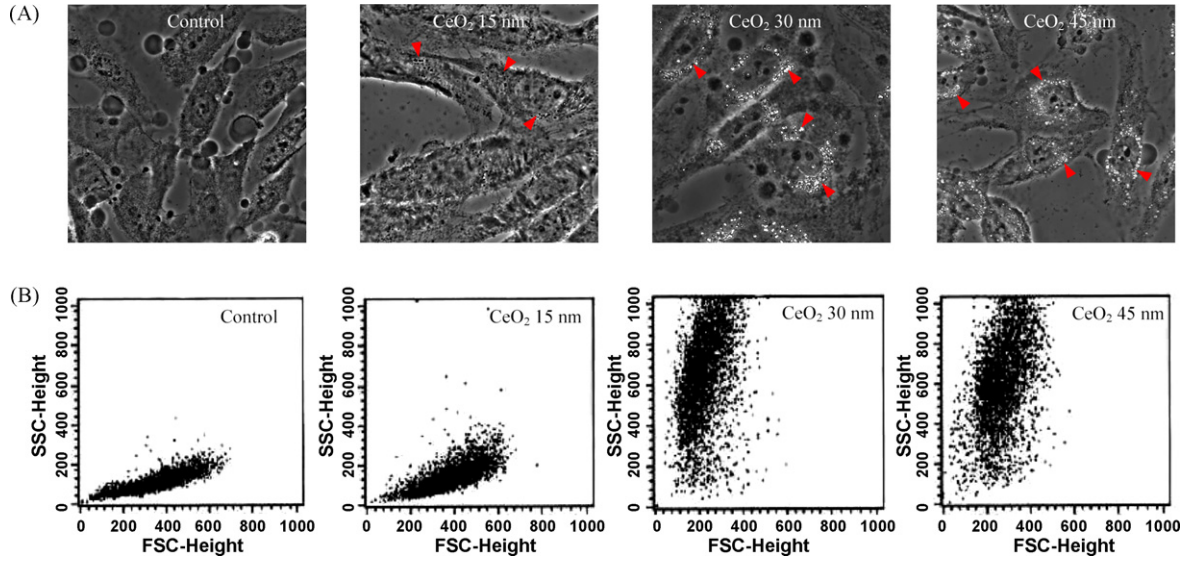

Fig. 2. Confocal reflectance image (A) and flow cytometric histograms of FS and SS (B) observed in the cells exposed to different sized CeO_2 nanoparticles for 24 h. Aggregates of CeO_2 nanoparticles in the cells were visualized using confocal LSM. FS and SS analysis using FCM suggested the incorporation of CeO_2 nanoparticles into the cells.

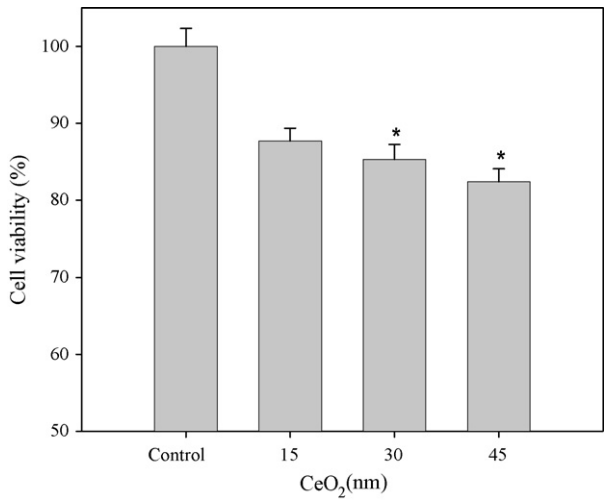

Fig. 3. The effect of different sized CeO_2 nanoparticles on the cell viability using the MTT assay. Results are presented in relative units compared to the control. Data represent the mean ± standard error of the mean of three individual experiments. $^*p < 0.05$ compared to the control group.

concentration of ROS in CeO_2 treated cells, however, a quantification analysis did not indicate any size-dependant effect.

To understand the mechanism of oxidative stress due to exposure to CeO_2 nanoparticles (Park et al., 2008), the detection of molecular events, such as MAP kinases signal transduction and subsequent transcription factor activation (Fig. 5), were undertaken. The expressions of the unphosphorlyated forms of MAP kinases were constant, regardless of the exposure to CeO_2 nanoparticles in all three kinases; whereas, the phosphorylation of p38 was most significantly induced by all three CeO_2 nanoparticle sizes (about 7–10-fold compared with that of the control). The phosphorylation of ERK and JNK induced by CeO_2 nanoparticles was hardly observed. The overall results for ROS formation (Fig. 4) and on MAP kinases signaling studies (Fig. 5) suggested that CeO_2 nanoparticles provoke oxidative stress and in response to this, mainly the p38 MAP kinase signaling pathway seems to be activated.

As a downstream event of MAP kinases signaling, NF-κB and Nrf-2, transcription factors, which are known to respond to oxidative stress, were examined in the cytosolic and nuclear fraction of cells treated with CeO_2 nanoparticles (Fig. 6). CeO_2 nanoparticles induced neither the nuclear localization of the NF-κB 65 kDa subunit nor the degradation of cytosolic I-κB. Therefore, the more recently characterized redox-sensitive transcription factor, Nrf-2, was investigated as a target of CeO_2 nanoparticles toxicity. CeO_2 nanoparticles induced the translocation of Nrf-2 into the nucleus, as evidenced by the results of the western blot analysis (Fig. 6).

To further investigate the cellular consequences of oxidative stress signaling through p38-Nrf-2 activation by CeO_2 nanoparticles exposure, representative antioxidant enzymes, such as, the expressions of SOD and HO-1 were examined (Fig. 7). SOD is a

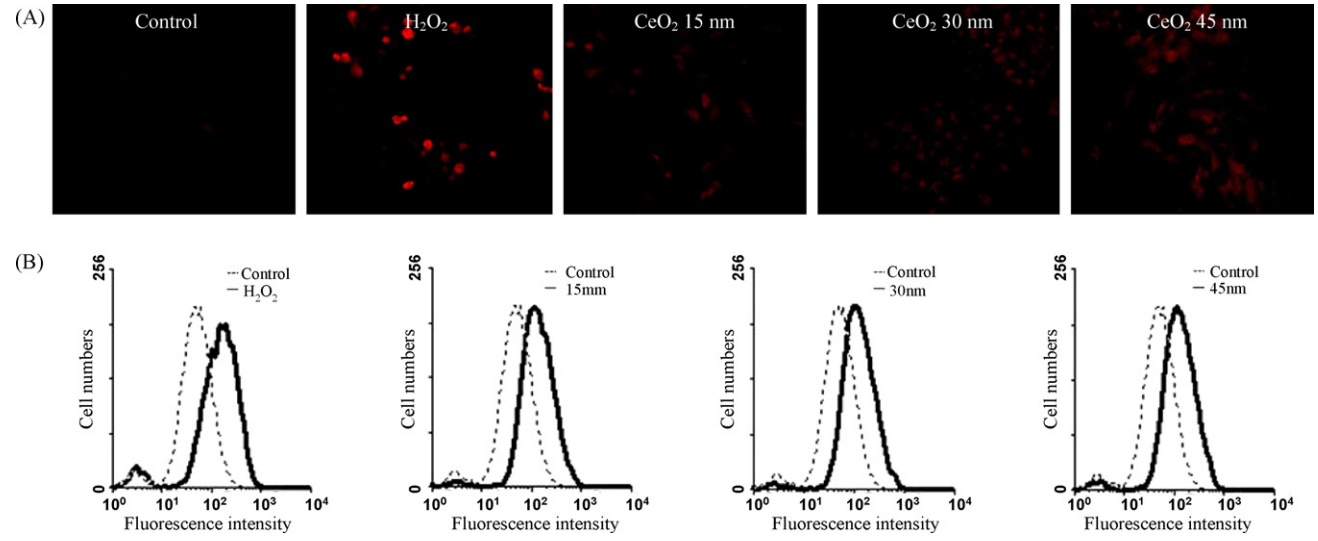

Fig. 4. ROS induced by nanoparticles in Beas-2B cells. The cells were incubated with different sized CeO_2 nanoparticles for 24 h and 40 μM DCFH-DA at 37 °C for 30 min and observed using fluorescence microscopy (A). H_2O_2 (100 μM) was used as the positive control. The fluorescence intensity of the cells was quantified by FCM analysis (B).

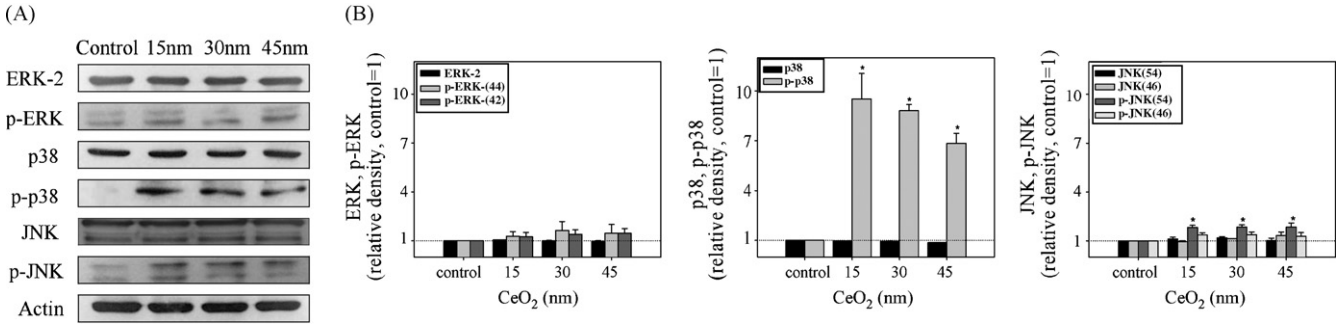

Fig. 5. The expressions of intact and phosphorylated ERK, p38 and JNK in Beas-2B cells exposed to different sized CeO_2 nanoparticles for 24 h (A). Densitometric values for the expressions of ERK, p38 and JNK were normalized using that of actin, and presented as relative units compared to the control. Data represent the mean ± standard error of the mean of three individual experiments. $^*p < 0.05$ compared to the control group (B).

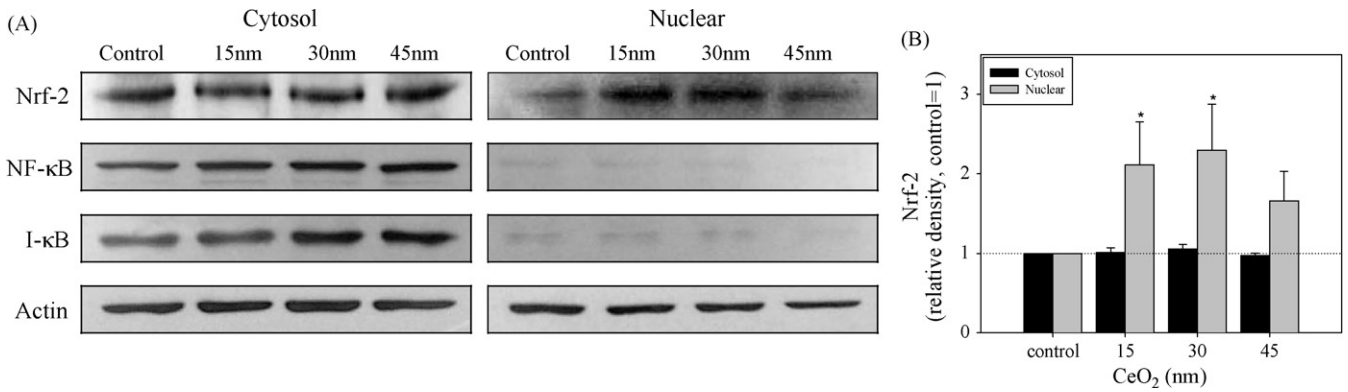

Fig. 6. Expressions of NF-κB, I-κB and Nrf-2 in cytosolic and nuclear fractions of Beas-2B cells exposed to different sized CeO_2 nanoparticles for 24 h (A). Densitometric values for the expression of Nrf-2 were normalized using that of actin, and presented as relative units compared to the control. Data represent the mean ± standard error of the mean of three individual experiments. $^*p < 0.05$ compared to the control group (B).

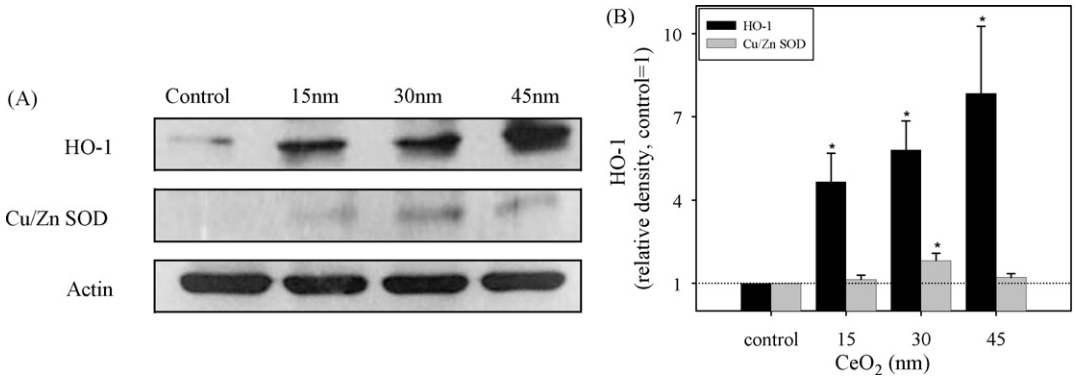

Fig. 7. The expressions of HO-1 and Cu/Zn SOD in Beas-2B cells exposed to different sized CeO_2 nanoparticles for 24 h (A). Densitometric values for the expressions of HO-1 and Cu/Zn SOD were normalized using that of actin, and presented as relative units compared to the control. Data represent the mean ± standard error of the mean of three individual experiments. $^*p < 0.05$ compared to the control group (B).

well-characterized primary enzyme for ROS scavenging; whereas, HO-1 is a relatively novel enzyme, with potent anti-inflammatory and cytoprotective antioxidant effects (Maines, 1988; Morse and Choi, 2002; Otterbein et al., 2003; Chen et al., 2005; Lee and Surh, 2005). The expression of HO-1 protein was dramatically increased in CeO_2 nanoparticles-treated cells (about 4–7-fold compared with that of the control). Conversely, no increase in the expression of SOD protein was observed due to exposure to CeO_2 nanoparticles. The increase was the most significant with exposure to the 45 nm CeO_2 nanoparticles. The induction of HO-1 due to expose to CeO_2 nanoparticles may be mediated through p38 MAP kinase (Fig. 5) and the Nrf-2 signal transduction pathway (Fig. 6). Recently, Lim et al. (2007) reported that the cyclopentenone prostaglandin compound stimulates HO-1 expression through the p38 MAP kinase and Nrf-2 pathway in rat vascular smooth muscle cells. Induction of HO-1 can be interpreted as a cellular defense mechanism against oxidative stress; it is well known that HO-1 induction is regulated by Nrf-2 activation (Itoh et al., 2003). In this study, CeO_2 nanoparticles-induced NF-κB activation was not observed, which was unexpected, as NF-κB is the major stress response transcription factor, and has been reported to respond to a wide variety of environment stressors. Therefore, although no CeO_2-induced NF-κB activation was observed in this study, the relative importance of NF-κB *vs*. Nrf-2 signaling in terms of a contribution to antioxidant response, such as HO-1 up regulation, may merit further investigation with various oxidative stress-inducing nanoparticles.

Moreover, CeO_2 nanoparticles-induced oxidative stress seems to result in apoptosis, where the number of cells localized in the subdiploid DNA peak was significantly increased compared with that of the control (Fig. 8). The degree of this increase in the number of cells localized in the subdiploid due to CeO_2 exposure was about 2–8-fold compared to that of the control. Cytosolic caspase-3

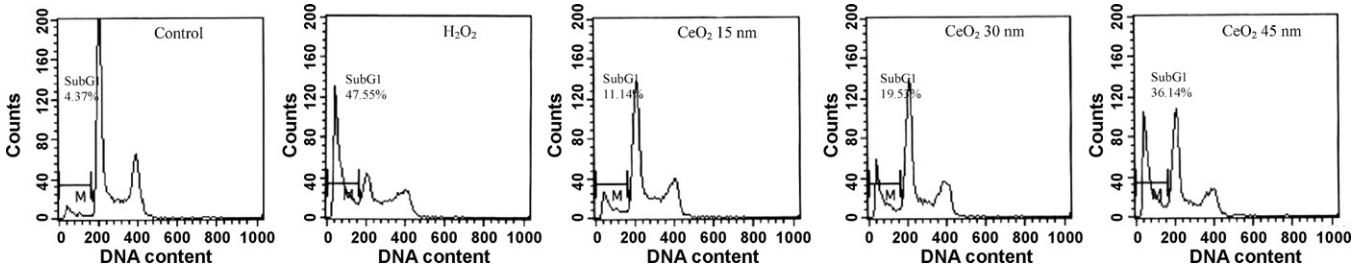

Fig. 8. Flow cytometric analysis to quantify the number of cells with a subdiploid DNA content in Beas-2B cells exposed to CeO_2 nanoparticles (15, 30 and 45 nm). H_2O_2 (100 μM) was used as the positive control.

and chromatin condensation by CeO_2 nanoparticles have previously been observed as indices of apoptosis (Park et al., 2008).

Smaller sized nanoparticles are often expected to exert stronger toxicity (Oberdörster et al., 2005). The particle size and surface area are considered important factors for determining the toxicity of nanoparticles, because, as the particle size decreases the surface area increases. In the present study, the hypothesis that "the cytotoxicity of nanoparticles is related to their surface area" was tested by assessing the toxicity of nanoparticles of the same material, but with different sizes. However, no size-dependant response was observed in this study. Unexpectedly, for HO-1 induction and the number of cells in subG1 phase, the 45 nm CeO_2 nanoparticles caused the most significant responses. Nevertheless, to confirm the size-dependent effect in CeO_2 nanoparticles-induced toxicity, further experiments on various sized nanoparticles with various exposure periods may be required, because it is also believed that parameters other than size (i.e. shape, charge, concentration, etc.) may also influence the toxicity of these nanoparticles. Most studies have failed to show any clear relationship between cytotoxicity and nanoparticle size (Hussain et al., 2005; Yin et al., 2005). Moreover, comparative experiments, including non-nanoscale CeO_2, need to be conducted to confirm the observed toxicities were due to the nanoscaled CeO_2, which are ongoing in our laboratory.

Overall, our results suggest that CeO_2 nanoparticles may exert their toxicity through oxidative stress. They cause a significant increase in cellular ROS concentrations, and subsequently lead to a strong induction of HO-1 *via* the p38-Nrf-2 signaling pathway. The tested oxidative stress parameters in this study were rather limited in terms of allowing a full understanding of the oxidative stress and cellular response due to exposure to CeO_2 nanoparticles. Further studies on the mechanism by which CeO_2 nanoparticles induce the p38-Nrf-2 signaling pathway to better understand the CeO_2 nanoparticles-induced oxidative stress, as well as with concentration–response and time-course analyses are warranted.

Conflict of interest

The authors have nothing to declare.

Acknowledgment

This subject is supported by Korea Ministry of Environment as "The Eco-technopia 21 project".

Appendix A. Supplementary data

Supplementary data associated with this article can be found, in the online version, at doi:10.1016/j.toxlet.2009.01.028.

References

Braydich-Stolle, L., Hussain, S., Schlager, J.J., Hofmann, M.C., 2005. In vitro cytotoxicity of nanoparticles in mammalian germline stem cells. Toxicol. Sci. 88, 412–419.

Camacho-Barquero, L., Villegas, I., Sánchez-Calvo, J.M., Talero, E., Sánchez-Fidalgo, S., Motilva, V., Alarcón de la Lastra, C., 2007. Curcumin, a Curcuma longa constituent, acts on MAPK p38 pathway modulating COX-2 and iNOS expression in chronic experimental colitis. Int. Immunopharmacol. 7, 333–342.

Chan, K., Han, X.D., Kan, Y.W., 2001. An important function of Nrf2 in combating oxidative stress: detoxification of acetaminophen. Proc. Natl. Acad. Sci. U.S.A. 98, 4611–4616.

Chan, K., Kan, Y.W., 1999. Nrf2 is essential for protection against acute pulmonary injury in mice. Proc. Natl. Acad. Sci. U.S.A. 96, 12731–12736.

Chen, C.Y., Jang, J.H., Li, M.H., Surh, Y.J., 2005. Resveratrol upregulates heme oxygenase-1 expression via activation of NF-E2-related factor 2 in PC12 cells. Biochem. Biophys. Res. Commun. 331, 993–1000.

Corma, A., Atienzar, P., Garcia, H., Chane-Ching, J.Y., 2004. Hierarchically mesostructured doped CeO_2 with potential for solar-cell use. Nat. Mater. 3, 394–397.

Elbekai, R.H., El-Kadi, A.O., 2005. The role of oxidative stress in the modulation of aryl hydrocarbon receptor-regulated genes by As^{3+}, Cd^{2+}, and Cr^{6+}. Free Radic. Biol. Med. 39, 1499–1511.

Foster, K.A., Galeffi, F., Gerich, F.J., Turner, D.A., Muller, M., 2006. Optical and pharmacological tools to investigate the role of mitochondria during oxidative stress and neurodegeneratation. Prog. Neurobiol. 79, 136–171.

Fotakis, G., Cemeli, E., Anderson, D., Timbrell, J.A., 2005. Cadmium chloride-induced DNA and lysosomal damage in a hepatoma cell line. Toxicol. In Vitro 19, 481–489.

Green, M., Howman, E., 2005. Semiconductor quantum dots and free radical induced DNA nicking. Chem. Commun. 121, 121–123.

Hagemann, C., Blank, J.L., 2001. The ups and downs of MEK kinase interactions. Cell Signal. 13, 863–875.

Hayes, J.D., Chanas, S.A., Henderson, C.J., McMahon, M., Sun, C., Moffat, G.J., Wolf, C.R., Yamamoto, M., 2000. The Nrf2 transcription factor contributes both to the basal expression of glutathione S-transferases in mouse liver and to their induction by the chemopreventive synthetic antioxidants, butylated hydroxyanisole and ethoxyquin. Biochem. Soc. Trans. 28, 33–41.

Hussain, S.M., Hess, K.L., Gearhart, J.M., Geiss, K.T., Schlager, J.J., 2005. In vitro toxicity of nanoparticles in BRL 3A rat liver cells. Toxicol. In Vitro 19, 975–983.

Itoh, K., Chiba, T., Takahashi, S., Ishii, T., Igarashi, K., Katoh, Y., Oyake, T., Hayashi, N., Satoh, K., Hatayama, I., Yamamoto, M., Nabeshima, Y., 1997. An Nrf2/small Maf heterodimer mediates the induction of phase II detoxifying enzyme genes through antioxidant response elements. Biochem. Biophys. Res. Commun. 236, 313–322.

Itoh, K., Wakabayashi, N., Katoh, Y., Ishii, T., O'connor, T., Yamamoto, M., 2003. Keap1 regulates both cytoplasmic–nuclear shuttling and degradation of Nrf2 in response to electrophiles. Genes Cells 8, 379–391.

Izu, N., Shin, W., Matsubara, I., Murayama, N., 2004. Development of resistive oxygen sensors based on cerium oxide thick film. J. Electroceram. 13, 703–706.

Janssen, Y.M., Barchowsky, A., Treadwell, M., Driscoll, K.E., Mossman, B.T., 1995. Asbestos induces nuclear factor kappa B (NF-kappa B) DNA-binding activity and NF-kappa B-dependent gene expression in tracheal epithelial cells. Proc. Natl. Acad. Sci. U.S.A. 92, 8458–8462.

Kim, Y.C., Masutani, H., Yamaguchi, Y., Itoh, K., Yamamoto, M., Yodoi, J., 2001. Hemin-induced activation of the thioredoxin gene by Nrf2. A differential regulation of the antioxidant responsive element by a switch of its binding factors. J. Biol. Chem. 276, 18399–18406.

Kwak, M.K., Itoh, K., Yamamoto, M., Kensler, T.W., 2002. Enhanced expression of the transcription factor Nrf2 by cancer chemopreventive agents: role of antioxidant response element-like sequences in the nrf2 promoter. Mol. Cell. Biol. 22, 2883–2892.

Kyriakis, J.M., Avruch, J., 2001. Mammalian mitogen-activated protein kinase signal transduction pathways activated by stress and inflammation. Physiol. Rev. 81, 807–869.

Lam, C.W., James, J.T., McCluskey, R., Hunter, R.L., 2004. Pulmonary toxicity of single-wall carbon nanotubes in mice 7 and 90 days after intratracheal instillation. Toxicol. Sci. 77, 126–134.

Lee, J.S., Surh, Y.J., 2005. Nrf2 as a novel molecular target for chemoprevention. Cancer Lett. 224, 171–184.

Lim, H.J., Lee, K.S., Lee, S., Park, J.H., Choi, H.E., Go, S.H., Kwak, H.J., Park, H.Y., 2007. 15d-PGJ2 stimulates HO-1 expression through p38 MAP kinase and Nrf-2 pathway in rat vascular smooth muscle cells. Toxicol. Appl. Pharmacol. 223, 20–27.

Limbach, L.K., Wick, P., Manser, P., Grass, R.N., Bruinink, A., Stark, W.J., 2007. Exposure of engineered nanoparticles to human lung epithelial cells: influence of chemical composition and catalytic activity on oxidative stress. Environ. Sci. Technol. 41, 4158–4163.

Lin, W., Huang, Y.W., Zhou, X.D., Ma, Y., 2006. Toxicity of cerium oxide nanoparticles in human lung cancer cells. Int. J. Toxicol. 25, 451–457.

Maines, M.D., 1988. Heme oxygenase: function, multiplicity, regulatory mechanisms, and clinical applications. FASEB J. 2, 2557–2568.

Monteiller, C., Tran, L., MacNee, W., Faux, S., Jones, A., Miller, B., Donaldson, K., 2007. The pro-inflammatory effects of low-toxicity low-solubility particles, nanoparticles and fine particles, on epithelial cells in vitro: the role of surface area. Occup. Environ. Med. 64, 609–615.

Monteiro-Riviere, N.A., Nemanich, R.J., Inman, A.O., Wang, Y.Y., Riviere, J.E., 2005. Multi-walled carbon nanotube interactions with human epidermal keratinocytes. Toxicol. Lett. 155, 377–384.

Morse, D., Choi, A.M., 2002. Heme oxygenase-1: the "emerging molecule" has arrived. Am. J. Respir. Cell Mol. Biol. 27, 8–16.

Mosmann, T., 1983. Rapid colorimetric assay for cellular growth and survival: application to proliferation and cytotoxicity assays. J. Immunol. Methods 16, 55–63.

Murray, E.P., Tsai, T., Barnett, S.A., 1999. A direct methane fuel cell with a ceria based a node. Nature 400, 649–651.

Oberdörster, E., 2004. Manufactured nanomaterials (fullerenes, C60) induce oxidative stress in the brain of juvenile largemouth bass. Environ. Health Perspect. 112, 1058–1062.

Oberdörster, G., Oberdörster, E., Oberdörster, J., 2005. Nanotoxicology: an emerging discipline evolving from studies of ultrafine particles. Environ. Health Perspect. 113, 823–839.

Otterbein, L.E., Soares, M.P., Yamashita, K., Bach, F.H., 2003. Heme oxygenase-1: unleashing the protective properties of heme. Trends Immunol. 24, 449–455.

Park, E.J., Choi, J., Park, Y.K., Park, K., 2008. Oxidative stress induced by cerium oxide nanoparticles in cultured BEAS-2B cells. Toxicology 245, 90–100.

Park, S.Y., Lee, S.M., Ye, S.K., Yoon, S.H., Chung, M.H., Choi, J., 2006. Benzo[a]pyrene-induced DNA damage and p53 modulation in human hepatoma HepG2 cells for the identification of potential biomarkers for PAH monitoring and risk assessment. Toxicol. Lett. 167, 27–33.

Pinkus, R., Weiner, L.M., Daniel, V., 1996. Role of oxidants and antioxidants in the induction of AP-1, NF-kappaB, and glutathione S-transferase gene expression. J. Biol. Chem. 271, 13422–13429.

Qadri, I., Iwahashi, M., Capasso, J.M., Hopken, M.W., Flores, S., Schaack, J., Simon, F.R., 2004. Induced oxidative stress and activated expression of manganese superoxide dismutase during hepatitis C virus replication: role of JNK, p38 MAPK and AP-1. Biochem. J. 378, 919–928.

Sayes, C.M., Gobin, A.M., Ausman, K.D., Mendez, J., West, J.L., Colvin, V.L., 2005. Nano-C60 cytotoxicity is due to lipid peroxidation. Biomaterials 26, 7587–7595.

Schubert, D., Dargusch, R., Raitano, J., Chan, S.W., 2006. Cerium and yttrium oxide nanoparticles are neuroprotective. Biochem. Biophys. Res. Commun. 342, 86–91.

Sen, C.K., Packer, L., 1996. Antioxidant and redox regulation of gene transcription. FASEB J. 10, 709–720.

Shvedova, A.A., Castranova, V., Kisin, E.R., Schwegler-Berry, D., Murray, A.R., Gandelsman, V.Z., Maynard, A., Baron, P.J., 2003. Exposure to carbon nanotube material: assessment of nanotube cytotoxicity using human keratinocyte cells. J. Toxicol. Environ. Health A 66, 1909–1926.

Suzuki, H., Toyooka, T., Ibuki, Y., 2007. Simple and easy method to evaluate uptake potential of nanoparticles in mammalian cells using a flow cytometric light scatter analysis. Environ. Sci. Technol. 41, 3018–3024.

Takeda, K., Matsuzawa, A., Nishitoh, H., Ichijo, H., 2003. Roles of MAPKKK ASK1 in stress-induced cell death. Cell Struct. Funct. 28, 23–29.

Xia, T., Korge, P., Weiss, J.N., Li, N., Venkatesen, M.I., Sioutas, C., Nel, A., 2004. Quinones and aromatic chemicals compounds inparticulate matter induce mitochondrial dysfunction: implications for ultrafine particle toxicity. Environ. Health Perspect. 112, 1347–1358.

Yin, H., Too, H.P., Chow, G.M., 2005. The effects of particle size and surface coating on the cytotoxicity of nickel ferrite. Biomaterials 26, 5818–5826.

Zheng, X., Zhang, X., Wang, X., Wang, S., Wu, S., 2005. Preparation and characterization of CuO/CeO_2 catalysts and their applications in low-temperature CO oxidation. Appl. Catal. A: Gen. 295, 142–149.